Oscillator death induced by amplitude-dependent coupling in repulsively coupled oscillators

Weiqing Liu,[1,2] Guibao Xiao,[1] Yun Zhu,[1] Meng Zhan,[3,*] Jinghua Xiao,[4] and Jürgen Kurths[5,6]

[1]*School of Science, Jiangxi University of Science and Technology, Ganzhou 341000, People's Republic of China*

[2]*State Key Laboratory of Magnetic Resonance and Atomic and Molecular Physics, Wuhan Institute of Physics and Mathematics, Chinese Academy of Sciences, Wuhan 430071, China*

[3]*State Key Laboratory of Advanced Electromagnetic Engineering and Technology, School of Electrical and Electronic Engineering, Huazhong University of Science and Technology, Wuhan 430074, China*

[4]*School of Science, Beijing University of Posts and Telecommunications, Beijing 100876, China*

[5]*Institute of Physics, Humboldt University Berlin, Berlin D-12489, Germany*

[6]*Potsdam Institute for Climate Impact Research, Telegraphenberg, Potsdam D-14415, Germany*

(Received 19 October 2014; published 7 May 2015)

The effects of amplitude-dependent coupling on oscillator death (OD) are investigated for two repulsively coupled Lorenz oscillators. Based on numerical simulations, it is shown that as constraint strengths on the amplitude-dependent coupling change, an oscillatory state may undergo a transition to an OD state. The parameter regimes of the OD domain are theoretically determined, which coincide well with the numerical results. An electronic circuit is set up to exhibit the transition process to the OD state with an amplitude-dependent coupling. These findings may have practical importance on chaos control and oscillation depression.

DOI: 10.1103/PhysRevE.91.052902 PACS number(s): 05.45.Xt, 05.65.+b

I. INTRODUCTION

Coupled dynamical systems often exhibit rich forms of emergent phenomena [1–3]. Besides synchronization as one of the major self-organized behaviors [4–6], oscillation quenching [7–9] refers to a suppression of oscillation under various types of interaction or intentional control. Two kinds of oscillation quenching including amplitude death (AD) and oscillation death (OD) have been extensively studied in many real-world applications, such as vibration suppression in mechanical engineering [10], synthetic genetic networks [11,12], and laser systems [13,14]. The key characters and differences between these two types of oscillation quenching are as follows. The AD suppresses oscillations through the occurrence of a single stable homogeneous steady state (HSS) and thus it is mainly applied as a control tool in coupled systems [15,16]. In contrast, the OD appears showing a stable inhomogeneous steady state (IHSS) owing to a symmetry breaking of the system. Thus, the OD is much more significant for life science compared to AD; for example, it can provide an essential mechanism for cellular differentiation [17,18]. Very recently, it has been verified that AD may transit to OD via a Turing-type bifurcation due to the interplay between the heterogeneity of the coupled oscillators and the coupling strength [9], or via repulsive interaction [19,20]. In addition, in the context of network topologies, oscillation quenching has been studied for regular networks such as global (all-to-all) [21] or local coupling [22,23], and networks with complex topologies such as small-world networks [24] or scale-free networks [25,26]. In general, the mechanisms for the appearance of OD are related to the characteristics of either the interacting units (such as frequency mismatches [21,27] and the spatial distributions of parameter mismatches [28,29]), or the coupling schemes [such as dissimilar (or conjugate) variables coupling [7,30,31], dynamical coupling [32], repulsive coupling [19,20], and delayed time coupling [33–36], etc.].

So far little attention has been on the characteristics of transferring interaction signals between coupled oscillators. In many realistic systems, the amplitude-frequency and phase-frequency characteristics of the coupling unit are very important since they have significant influences on the dynamical process. The amplitude constraint effect, as one of the amplitude-phase characteristics, refers to signals whose amplitude is larger than a limitation and have to saturate to a limited value, could have significant influence on the signals transferring results. For instance, in electronic engineering limiting amplifiers [37] were invented and have been widely applied to various forms of communication systems such as optical fiber communication [38], digital communication, and microwave communication. In some theoretic studies, Gao *et al.* [39] found that a single chaotic system can be controlled to various target states such as periodic or steady states when applying the amplitude constraint on a single variable. In addition, spatiotemporal chaos can also be tamed to stationary patterns if some transferring signals are repressed, with the so-called phase space compression method [40]. Therefore, it is meaningful to explore amplitude constraint effects in more general dynamical systems point of view, such as studying the model of two coupled chaotic oscillators, and make a connection with the OD phenomenon. In this paper, we investigate amplitude-dependent coupling effects on OD by studying the repulsively coupled chaotic or periodic oscillators experimentally and numerically, and we find solid evidence that there is an optimal level of amplitude constraint which can force the coupled oscillators to damp.

II. MODELS

Let us consider two diffusively coupled oscillators with amplitude constraint effects,

$$\dot{X}_1(t) = f(X_1(t)) + \epsilon_2 U_1(t),$$
$$\dot{X}_2(t) = f(X_2(t)) + \epsilon_2 U_2(t), \quad U_2(t) = -U_1(t),$$

*zhanmeng@wipm.ac.cn

$$U_1(t) = \begin{cases} \Gamma U_C, & \epsilon_1 \Gamma[X_2(t) - X_1(t)] \geqslant U_C \\ \epsilon_1 \Gamma[X_2(t) - X_1(t)], & |\epsilon_1 \Gamma[X_2(t) - X_1(t)]| \leqslant U_C \\ -\Gamma U_C, & \epsilon_1 \Gamma[X_2(t) - X_1(t)] \leqslant -U_C \end{cases}, \tag{1}$$

where $X_i \in R^n (i = 1,2)$, $f : R^n \to R^n$ represents a nonlinear function capable of exhibiting rich dynamics including chaos, ϵ_2 is a scalar control coupling strength, and $U_{1,2}$ denotes an interaction signal transferred. Since the coupling terms U_i are strongly related to the amplitude of the input signals, we name it amplitude-dependent coupling. Here the variable ϵ_1 is the amplifying coefficient of the coupling unit, Γ is a constant matrix describing the coupling scheme, and U_C ($U_C > 0$) is the amplitude constraint constant of the coupling unit with which all signals larger than U_C (or less than $-U_C$) are confined to U_C (or $-U_C$), whereas when the maximal amplitudes of signal in the coupling unit are less than U_C ($|\epsilon_1 \Gamma[X_2(t) - X_1(t)]| < U_C$), there are no amplitude constraint effects. To explore the amplitude-dependent coupling induced OD in the coupled system, it is convenient to analyze the existence and stability of the corresponding OD state.

Let $\dot{X}_i(t) = 0$; the fixed point (X_1^*, X_2^*) could be determined by the following equations:

$$f(X_1^*) + \epsilon_2 U_1 = 0, \quad f(X_2^*) + \epsilon_2 U_2 = 0. \tag{2}$$

If $U_2 = -U_1$ and f is an odd function of X, i.e., $f(-X) = -f(X)$, Eqs. (2) can be further combined to a single equation,

$$f(X_1^*) + \epsilon_2 U_1 = 0. \tag{3}$$

Then the fixed points (X_1^*, X_2^*) ($X_2^* = -X_1^*$) can be classified according to the different values of U_C:

(i) If U_C is sufficiently large ($|2\epsilon_1 \Gamma X_1^*| < U_C$) and there is no amplitude constraint effect, then X_1^* is determined by

$$f(X_1^*) - 2\epsilon_2 \epsilon_1 \Gamma X_1^* = 0. \tag{4}$$

(ii) If U_C is sufficiently small ($|2\epsilon_1 \Gamma X_1^*| > U_C$), then

$$f(X_1^*) + \epsilon_2 \Gamma U_C = 0. \tag{5}$$

With no amplitude constraint in case (i), the stability of the fixed point has been discussed in Ref. [20] and the stable OD can be observed for a suitably selected repulsive coupling. In contrast, with the amplitude constraint in case (ii), the stability of the fixed point can be determined by the linearization analysis. Letting $X_i = X_i^* + \eta_i$ ($i = 1,2$) and linearizing Eq. (1) around X_i^*, we obtain

$$\begin{pmatrix} \dot{\eta}_1 \\ \dot{\eta}_2 \end{pmatrix} = \begin{pmatrix} D\mathbf{f}(\mathbf{X}_1^*) & 0 \\ 0 & D\mathbf{f}(-\mathbf{X}_1^*) \end{pmatrix} \begin{pmatrix} \eta_1 \\ \eta_2 \end{pmatrix}. \tag{6}$$

Since $f(X)$ is an odd function of X, $Df(-X_1^*) = Df(X_1^*)$, Eq. (6) can be further simplified to

$$\dot{\eta}_i = D\mathbf{f}(\mathbf{X}_1^*)\eta_i, \quad i = 1,2. \tag{7}$$

Clearly the fixed point $(X_1^*, -X_1^*)$ becomes stable only when the maximal real part of the eigenvalues of $D\mathbf{f}(\mathbf{X}_1^*)$ is negative under the condition of the amplitude constraint ($|2\epsilon_1 \Gamma X_1^*| > U_C$).

III. OD IN COUPLED LORENZ SYSTEM

To explore OD in detail, let us employ a specific model of two repulsively coupled Lorenz systems. The equations of the classical chaotic Lorenz oscillator are

$$\begin{aligned} \dot{x_0}(t) &= \sigma(y_0(t) - x_0(t)), \\ \dot{y_0}(t) &= Rx_0(t) - y_0(t) - x_0(t)z_0(t), \\ \dot{z_0}(t) &= x_0(t)y_0(t) - bz_0(t). \end{aligned} \tag{8}$$

We have rescaled the variables $x_0(t), y_0(t), z_0(t)$ by the transformation of $x(t) = x_0(t)/5$, $y(t) = y_0(t)/5$, and $z(t) = z_0(t)/10$. Then the modified equations become

$$\begin{aligned} \dot{x}(t) &= \sigma[y(t) - x(t)], \\ \dot{y}(t) &= Rx(t) - y(t) - 10x(t)z(t), \\ \dot{z}(t) &= 2.5x(t)y(t) - bz(t), \end{aligned} \tag{9}$$

with the classical system parameters $\sigma = 10$, $R = 28$, and $b = 8/3$ for a chaotic oscillator. Note that the right hand side of Eqs. (9) satisfies the odd property for x and y, i.e., $f(-x, -y, z) = -f(x, y, z)$. We set the coupling scheme of two coupled Lorenz units

$$\Gamma = \begin{pmatrix} 0 & 0 & 0 \\ 0 & 1 & 0 \\ 0 & 0 & 0 \end{pmatrix},$$

then the coupling terms in Eqs. (2) become $\epsilon_2 U_1 = \epsilon_2 \epsilon_1 (y_2 - y_1)$ and $\epsilon_2 U_2 = \epsilon_2 \epsilon_1 (y_1 - y_2)$. If there is no amplitude constraint in the coupling unit (U_C is infinite), the coupled system may transit to complete synchronization with a positive ϵ ($\epsilon = \epsilon_2 \epsilon_1$) [4,41], or to antiphase synchronization otherwise [6], according to previous studies. Since the condition of amplitude constraint effects in the coupling unit is $U_C < |\epsilon_1 (y_2 - y_1)|_{\max}$, there should be no amplitude constraint effects if the complete synchronous ($y_2 = y_1$) happens [41]. Therefore, to make the effect more likely observable, we set $\epsilon_1 < 0$ and $\epsilon_2 > 0$.

To explore the stability of the OD state, let us first work out the fixed point with an amplitude constraint as $(X_1^*, X_2^*) = [x_1^*, x_1^*, 2.5(x_1^*)^2/b, -x_1^*, -x_1^*, 2.5(x_1^*)^2/b]$. According to Eqs. (5) and (9), x_1^* satisfies the equation $(R - 1)x - 25 * x^3/b + \epsilon_2 U_C = 0$, whose solution is

$$x_1^* = T/30 + \frac{2b(R-1)}{5T}, \tag{10}$$

with

$$T = \sqrt[3]{540\epsilon_2 U_C + 12b\sqrt{12b(1-R)^3 + 2025\epsilon_2^2 U_C^2}}. \tag{11}$$

Then its linearized matrix is presented as

$$Df(X_1^*) = \begin{pmatrix} -10 & 10 & 0 \\ R - (25/b)(x_1^*)^2 & -1 & -10x_1^* \\ 2.5x_1^* & 2.5x_1^* & -b \end{pmatrix}. \tag{12}$$

The eigenvalue λ_i's of $Df(X_1^*)$ can be obtained by using a symbolic manipulation program such as *Mathematica*. The expression of λ_i's are not presented here, since they are too complex and very long.

As a result, the stable OD domain of the coupled system should be determined by the following two key factors: (i) the parameter spaces when the maximal real part of the eigenvalue

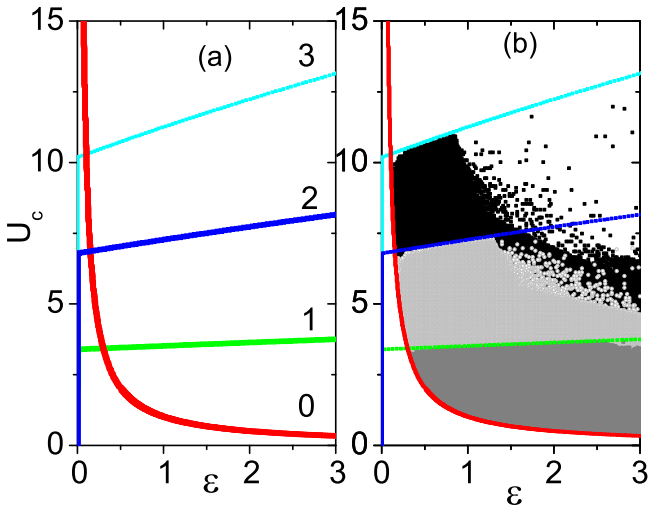

FIG. 1. (Color online) (a) The theoretical results of OD domains in the (ϵ_2-U_C) parameter space. The OD domain is enclosed by line 0 and lines $i, i = 1 - 3$ (above line 0 and below line i); the numbers 1–3 stand for $\epsilon_1 = -1, -2$, and -3, respectively. (b) The numerical results of OD domains marked by color dots with the same parameters as those in (a).

of the matrix [Eqs. (12)] is negative, and (ii) the parameter spaces by the amplitude constraint condition: $|2\epsilon_1 x_1^*| > U_C$, i.e., $U_C < \sqrt{(b/25)[8\epsilon_1^3\epsilon_2 + 4\epsilon_1^2(R-1)]}$. Figure 1(a) presents the critical lines of the stable OD according to these two factors. The line 0 corresponds to the critical line according to the factor (i), while the lines $i (i = 1, 2,$ and $3)$ are just the critical lines based on the factor (ii) for $\epsilon_1 = -1, -2$, and -3, respectively. The OD domains are the areas enclosed by the line 0 and the line i (areas above the line 0 and below the line i) for each $\epsilon_1 = -1, -2$, and -3, respectively. According to these theoretical results, it is obvious that there is an optimal interval of U_C which may lead to OD for a given set of ϵ_1 and ϵ_2. When U_C is large enough, the amplitude constraint does not have any impact and hence the dynamics is the same as that with ideal coupling. According to the results discussed in Ref. [6], there is no OD regime for this kind of repulsively coupled Lorenz system. On the contrary, if U_C is too small, the strong amplitude constraint cannot work either.

To verify our theoretical results, we calculate the dynamics of the coupled systems [Eqs. (9)] numerically. We record all parameters of ϵ_2 versus U_C when the coupled systems exhibit the OD state for random initial values. The parameter spaces of the OD state are dotted in black, light gray, and gray for $\epsilon_1 = -1, -2$, and -3, respectively, as shown in Fig. 1(b). We can find that the OD domains coincide well with the theoretical results when ϵ_2 is small, except that there are still some blank areas within the theoretically predicted OD domains left for possible oscillatory behaviors. By a careful check, we indeed find that the OD state coexists with the oscillating state within the blank areas. Figures 2(a) and 2(b) present two time series of $x_{1,2}(t)$ of the oscillating state and the OD state from different initial conditions. The oscillating state is in antiphase synchronization, which coincides with the finding in Ref. [6].

Since the OD and the oscillating states have their own attractor basins, the sizes of their basins should change for

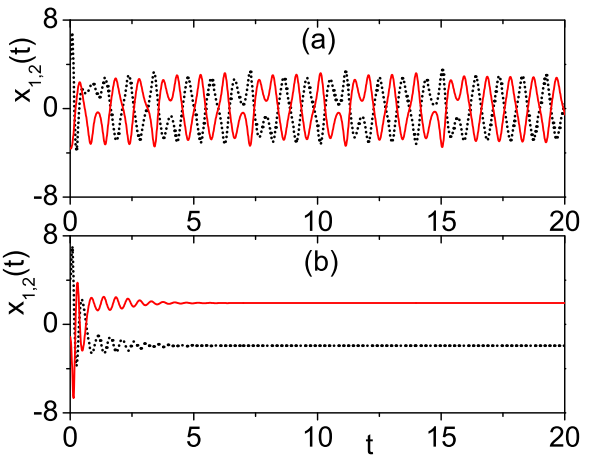

FIG. 2. (Color online) (a),(b) The time series of variable $x_{1,2}(t)$ for two coexisting solutions with two different initial value sets as (4.472 38, 5.005 78, − 1.994 34, − 3.600 81, − 3.7079, 3.139 42), (4.114 36,4.759 25, − 2.530 78, − 1.1519, − 2.7289, − 3.136 24), respectively; $\epsilon_1 = -2$, $\epsilon_2 = 3$, and $U_C = 5$.

different values of U_C. Figures 3(a)–3(c) present the basins of the OD states represented by dots for the parameters $U_C =$ 5, 6, and 6.5, respectively; $\epsilon_1 = -2$ and $\epsilon_2 = 3$. Obviously, the area of the OD basin shrinks with the value of U_C approaching the OD boundary in Fig. 1. We calculate the basin stability of the OD defined by $S_{\rm OD} = \frac{N_{\rm OD}}{N_{\rm tol}}$ [42], where $N_{\rm OD}$ denotes the number of sets of initial values leading to the OD state, while $N_{\rm tol} = 10\,000$ is fixed for all samples of initial values. If OD

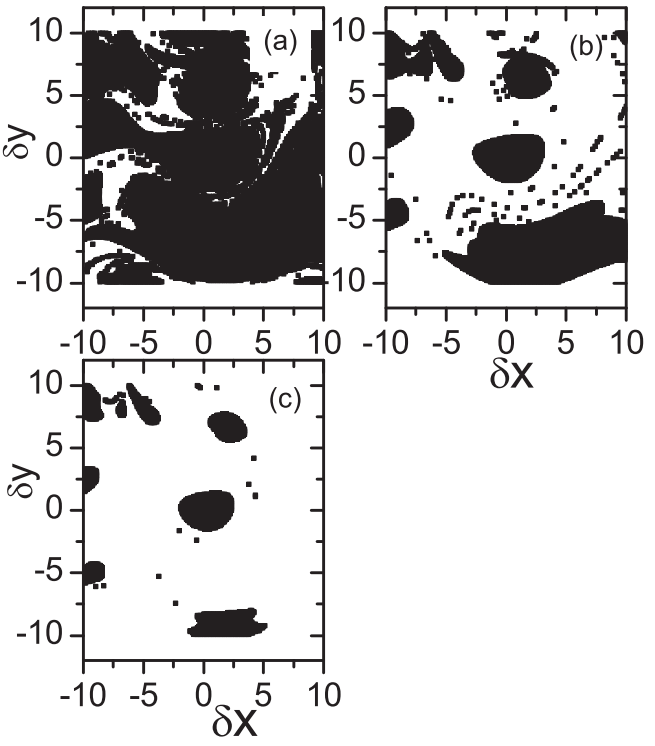

FIG. 3. (a)–(c) The basins of the OD states for $U_C = 5$, 6, and 6.5, respectively; $\epsilon_1 = -2$ and $\epsilon_2 = 3$. The initial value is set as $x_1 = y_1 = x_1^* + \delta x$, $x_2 = y_2 = -x_1^* + \delta y$, $z_1 = z_2 = (x_1^*)^2$, and all values of δx and δy are recorded when the OD state is finally achieved.

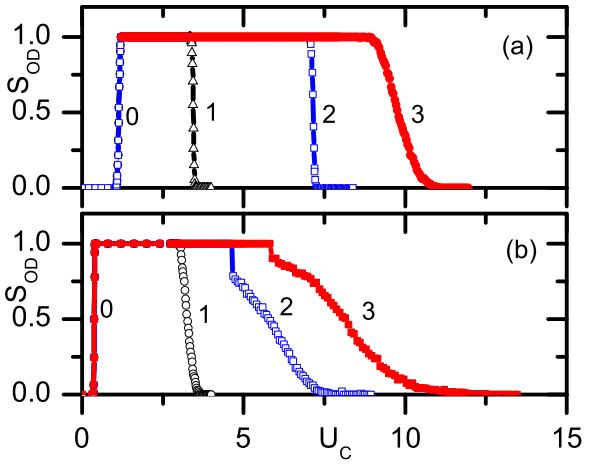

FIG. 4. (Color online) (a), (b) The basin stabilities of OD for $\epsilon_2 = 1$ and 3, respectively; $\epsilon_1 = -1$ (hollow triangle), -2 (hollow square), and -3 (solid square). The critical boundaries of U_C coincide with those in Fig. 1(a).

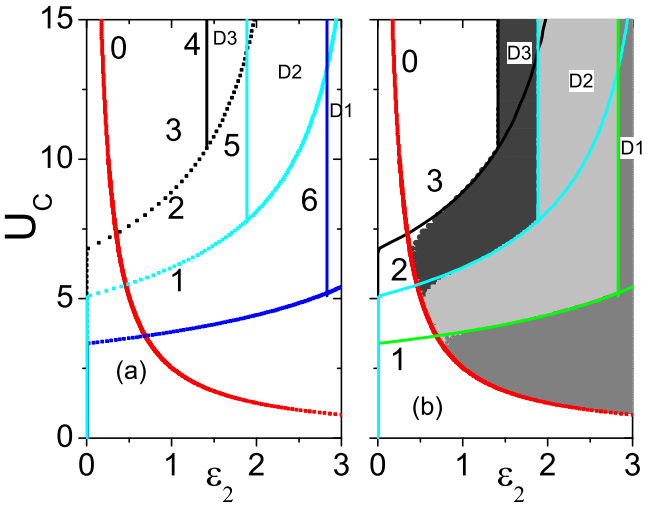

FIG. 5. (Color online) (a) The analytic results of the OD domains in the (ϵ_2-U_C) parameter space with a different coupling scheme considered [Eq. (13)]. The OD domains with the amplitude constraint effects are enclosed by line 0 and lines $i, i = 1-3$ (above line 0 and below lines i) for $\epsilon_1 = -1$, -1.5, and -2, respectively. The OD domains without the amplitude constraint effects are enclosed by lines 1 and 6, lines 2 and 5, and lines 3 and 4, for $\epsilon_1 = -1$, -1.5, and -2, respectively. (b) The numerical results compared with the analytic results in (a).

coexists with the oscillating state, $S_{\rm OD} \in (0,1)$, and otherwise if OD loses stability, $S_{\rm OD} = 0$. The results of $S_{\rm OD}$ for $\epsilon_2 = 1$ and 3 are presented in Figs. 4(a) and 4(b). We find that the critical values of U_C for $S_{\rm OD}$ jumping from 0 to 1 or decreasing from a finite value to 0 just match with the theoretical results in Fig. 1. To emphasize this point, we add 0, 1, 2, and 3 in the figures.

It is expected to observe amplitude-dependent coupling induced OD for other coupling schemes as well. Without losing generality, we consider the following coupling scheme:

$$\Gamma = \begin{pmatrix} 1 & 0 & 0 \\ 0 & 0 & 0 \\ 0 & 0 & 0 \end{pmatrix}. \tag{13}$$

If the coupling unit satisfies the condition of amplitude constraint $|2\epsilon_1 x_1^*| > U_C$ [Eq. (5)], we may obtain the fixed point $F_1(x_1^*, y_1^*, \frac{R(y_1^*+\epsilon_2 U_C/10)^2}{1+(y_1^*+\epsilon_2 U_C/10)^2}, -x_1^*, -y_1^*, \frac{R(y_1^*+\epsilon_2 U_C/10)^2}{1+(y_1^*+\epsilon_2 U_C/10)^2})$, where $x_1^* = y_1^* + \epsilon_2 U_C/10$, and $y_1^* = \frac{1}{30}\sqrt[3]{U_C^3\epsilon_2^3 + 6G + 18bU_C\epsilon_2 R + 36bU_C\epsilon_2} - \frac{30(-\frac{1}{900}U_C^2\epsilon_2^2 - \frac{bR}{75} + \frac{b}{75})}{\sqrt[3]{U_C^3\epsilon_2^3+6G+18bU_C\epsilon_2 R+36bU_C\epsilon_2}} - \frac{\epsilon_2 U_C}{15}$, with $G = \sqrt{3bU_C^4\epsilon_2^4 - 3b^2U_C^2\epsilon_2^2R^2 + 60b^2U_C^2\epsilon_2^2 r + 24b^2U_C^2\epsilon_2^2 - 48[b(R-1)]^3}$. The amplitude constraint condition becomes $|2\epsilon_1(y_1^* + \epsilon_2 U_C/10)| > U_C$, namely,

$$U_C < \frac{\epsilon_1\sqrt{b(\epsilon_2\epsilon_1 - 5)(-\epsilon_2\epsilon_1 - 5r + 5)}}{2.5(\epsilon_2\epsilon_1 - 5)}. \tag{14}$$

The linearized matrix is repressed as

$$Df(X_1^*) = \begin{pmatrix} -10 & 10 & 0 \\ R - \frac{25R(y_1^*+0.1\epsilon_2 U_c)^2/b}{1+25(y_1^*+0.1\epsilon_2 U_c)^2/b} & -1 & -10(y_1^* + 0.1\epsilon_2 U_c) \\ 2.5y_1^* & 2.5(y_1^* + 0.1\epsilon_2 U_c) & -b \end{pmatrix}. \tag{15}$$

Again the eigenvalues λ_i of $Df(X_1^*)$ are worked out by using *Mathematica*. One critical line (marked as line 0) of the OD domain is obtained when the largest real part of the eigenvalue is zero. Then the domain of OD induced by the amplitude constraint should be enclosed by the line 0 and the critical curves by Eq. (14).

However, on the other hand, if U_C is sufficiently large, $|2\epsilon_1 x_1^*| < U_C$, there is no amplitude constraint effect. We obtain the fixed point of the coupled Lorenz system as $F_2(x_1^*, \frac{bRx_1^*}{b+(x_1^*)^2}, -\frac{25Rx(x_1^*)^2}{10b+250(x_1^*)^2}, x_1^*, -\frac{bRx_1^*}{b+(x_1^*)^2}, \frac{25Rx(x_1^*)^2}{10b+250(x_1^*)^2})$ from Eq. (4). Thus x_1^* is determined by $\frac{\sigma bRx}{b+25x^2} - \sigma x - 2\epsilon_1\epsilon_2 x = 0$, i.e., $x_1^* = \sqrt{\frac{\sigma b(R-1) - 2\epsilon_1\epsilon_2 b}{25(\sigma+2\epsilon_1\epsilon_2)}}$. Based on the analysis in Ref. [20], we obtain that the fixed point is stable in the interval $\epsilon_1\epsilon_2 \in (-5, -2.83]$.

Finally, to combine these two components, the OD domain in the parameter space of U_C versus ϵ_2 consists of two types of OD domains: (i) The first one is the OD domain without

exhibiting the amplitude constraint effects, which is enclosed by the critical lines [Eq. (14)] and $\epsilon_1\epsilon_2 \in (-5, -2.83]$, and (ii) the second one is the OD domain showing the amplitude constraint effects, which are enclosed by the line 0 and the critical lines [Eq. (14)]. Again take $\epsilon_1 = -1,\ -2$, and -3 as examples; the OD domains of situation (i) are the areas enclosed by the lines 1 and 6 (D_1), lines 2 and 5 (D_2), and lines 3 and 4 (D_3), respectively, while those of situation (ii) are the areas enclosed by the lines 0 and 1, lines 0 and 2, and lines 0 and 3, respectively [see details in Fig. 5(a)]. The numerical results presented in Fig. 5(b) clearly coincide with the analytical results in Fig. 5(a). We also find that now there is no coexistence between the OD and the oscillating states, compared to the first coupling scheme.

IV. EXPERIMENTAL RESULTS

To experimentally observe the amplitude constraint effects, we set up the electronic circuit of the linearly coupled Lorenz system. The Lorenz circuit unit [43] is composed of three integrators, each realizing a variable of Lorenz equation, denoted by x_i, y_i, and z_i ($i = 1,2$), respectively. The nonlinear

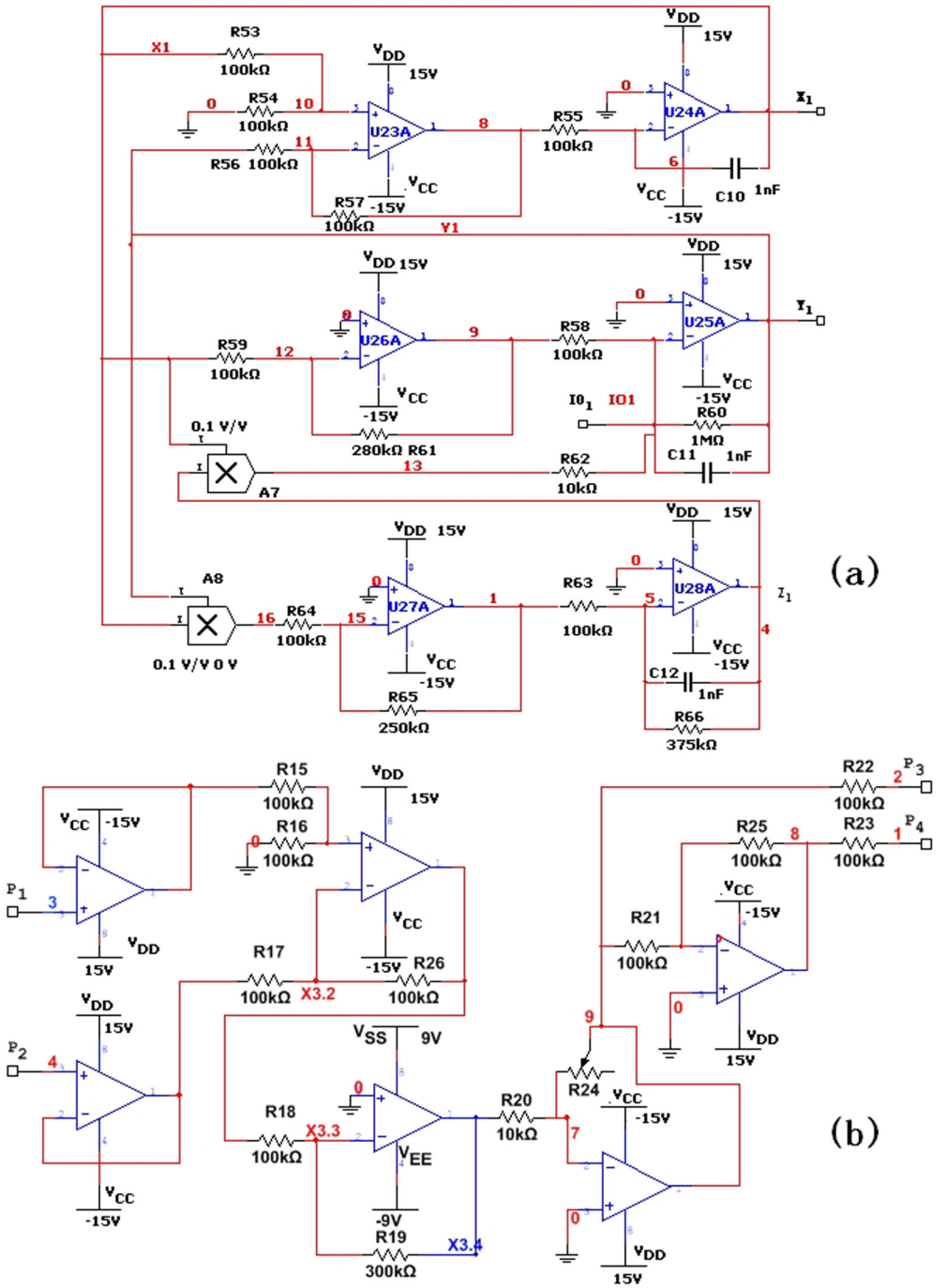

FIG. 6. (Color online) (a) The electronic circuit unit of a chaotic Lorenz oscillator. (b) The circuit of the coupling channel with the amplitude constraint effect. Here P_1 and P_2 are connected with X_1 of the two Lorenz circuit units, and P_3 and P_4 are connected with $I\,O_1$.

terms in the Lorenz equation are created by the analog multipliers (AD633/AD with a gain coefficient of 0.1), as shown in Fig. 6(a). The linear coupling unit in Fig. 6(b) can be set up based on an analog amplifier with an amplitude constraint effect. (Generally, the voltages of the source power of an analog amplifier are $V_{SS} = +15V$, $V_{EE} = -15V$, and the output signal is surely less than the limitation $|V_D| = |V_{SS}| - 1.5V$.) The unit consists of two obstructors, one subtractor, and three amplifiers (the two determine ϵ_1 and ϵ_2, and the other is with the gain of -1). Signals from y_1 (y_2) in the two Lorenz circuit units are input to P_1 (P_2) and transmitted to the places marked with IO_1 (IO_2) in Fig. 6(a) [and the duplicated Lorenz unit through P_4 (P_3)]. Thus, the coupled system can be described by

$$
\begin{aligned}
\dot{x_1}(t) &= \frac{1}{R_{55}C_{10}}[y_1(t) - x_1(t)],\\
\dot{y_1}(t) &= \frac{R_{61}}{R_{59}R_{58}C_{11}}x_1(t) - \frac{1}{R_{60}C_{11}}y_1(t)\\
&\quad - \frac{0.1}{R_{62}C_{11}}x_1(t)z_1(t) + \frac{R_{24}}{R_{20}}U(t),\\
\dot{z_1}(t) &= \frac{0.1R_{65}}{R_{64}R_{63}}x_1y_1(t) - \frac{1}{R_{66}C_{12}}z_1(t),\\
\dot{x_2}(t) &= \frac{1}{R_{55}C_{10}}[y_2(t) - x_2(t)],\\
\dot{y_2}(t) &= \frac{R_{61}}{R_{59}R_{58}C_{11}}x_2(t) - \frac{1}{R_{60}C_{11}}y_2(t)\\
&\quad - \frac{0.1}{R_{62}C_{11}}x_2(t)z_2(t) - \frac{R_{24}}{R_{20}}U(t),\\
\dot{z_2}(t) &= \frac{0.1R_{65}}{R_{64}R_{63}}x_2y_2(t) - \frac{1}{R_{66}C_{12}}z_2(t),\\
U(t) &= \frac{-R_{19}}{R_{18}}[y_2(t) - y_1(t)].
\end{aligned}
\tag{16}
$$

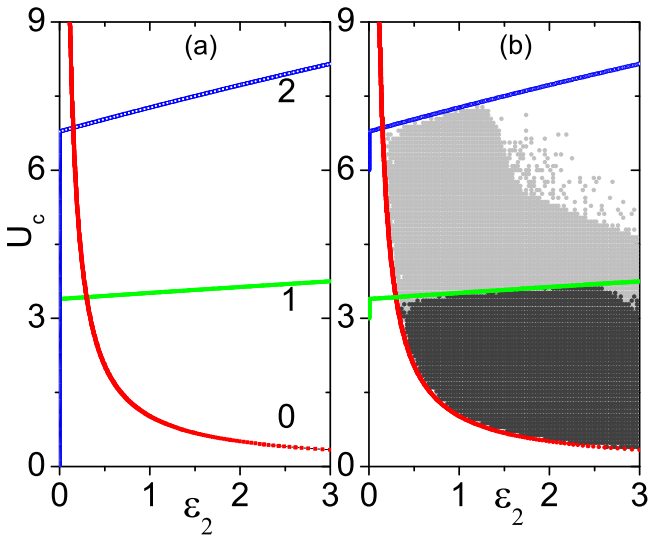

FIG. 7. (Color online) (a) Theoretical results of critical lines for OD domain in the (ϵ_2-U_C) parameter space with parameter $\epsilon_1 = -1$ (lines 0 and 1) and $\epsilon_1 = -2$ (lines 0 and 2), respectively. (b) The experimental results of OD domain for $\epsilon_1 = -1$ (light gray dots) and $\epsilon_1 = -2$ (dark gray dots), respectively.

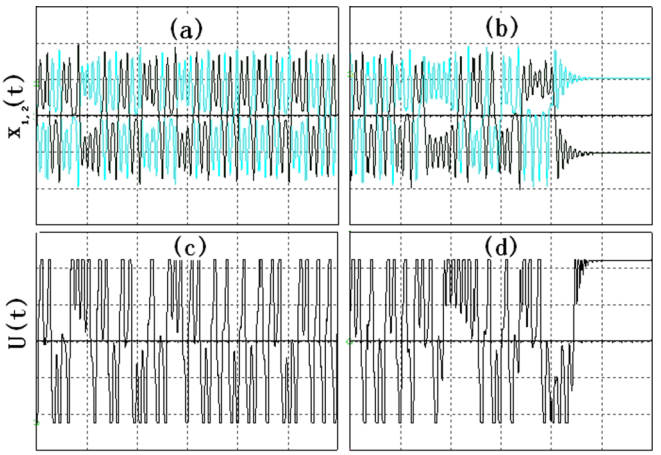

FIG. 8. (Color online) (a),(b) The time series of $x_{1,2}(t)$ of the coupled circuits for $R_{19} = 200$ K Ω ($\epsilon_2 = 3$) and $R_{24} = 3$ K Ω ($\epsilon_1 = -2$) showing the coexistence of the OD and oscillation for different initial conditions; $U_C \approx 4.5$ V and $V_{SS} = 6$ V. (c),(d) The corresponding $U(t)$'s in the channel of the coupled systems. The scales of the oscilloscope are 2 ms/division and 2 V/division.

Owing to the voltage limitation of the operational amplifier (OPAM), the output of the coupling unit $U(t)$ is not allowed to be larger than V_C. Otherwise, the OPAM will be saturated and have a constant output of $\pm V_C$. Therefore, by considering the amplitude constraint of the OPAM unit, we have

$$
U(t) = \begin{cases} V_C, & \frac{-R_{19}}{R_{18}}[y_2(t) - y_1(t)] > V_C \\ \frac{-R_{19}}{R_{18}}[y_2(t) - y_1(t)], & \left|\frac{-R_{19}}{R_{18}}[y_2(t) - y_1(t)]\right| \leqslant V_C; \\ -V_C, & \frac{-R_{19}}{R_{18}}[y_2(t) - y_1(t)] < -V_C \end{cases}
\tag{17}
$$

by changing the values of the resistor R_{19}, R_{24}, and the voltage of the OPAM [V_{SS} and V_{EE} in Fig. 6(b)], we can change the value of ϵ_1, ϵ_2, and the amplitude constraint strength V_C ($V_C \approx V_{SS} - 1.5V$) with $\epsilon_1 = -\frac{R_{19}}{R_{18}}$ and $\epsilon_2 = \frac{10R_{24}}{R_{20}}$ accordingly. Figure 7(b) presents the experimental results of the OD domain in the parameter space of ϵ_2 versus V_C, which coincide with the theoretical results in Fig. 7(a) and the numerical results in Fig. 1(b). Within the blank area in the stable OD domain predicted theoretically, the coexistence of the OD and oscillation states are also expected. By injecting electricity power to the capacity $C_1 \sim C_3$, we can change the initial values of the Lorenz circuit. The experimental results are shown in Figs. 8(a)–8(d), which record the time series of $x_{1,2}(t)$ and the corresponding $U(t)$'s within the two coexisting regimes for two sets of different initial values; the parameters are set as $\epsilon_1 = -2$ ($R_{18} = 100$ K Ω, $R_{19} = 200$ K Ω), $\epsilon_2 = 3$ ($R_{20} = 10$ K Ω, $R_{24} = 3$ K Ω), $V_{SS} = 6$ V, and $V_{EE} = -6$ V.

V. CONCLUSION

By considering the amplitude constraint effect of the coupling unit, we have found that two repulsively coupled chaotic oscillators can undergo a transition from oscillation to OD for properly selected control parameters. This amplitude constraint induced OD is of general importance because the

coupling units usually have a limitation of the signal amplitude in many realistic systems. Since the signal transferring in the coupling unit is larger than the limitation, the signal will be saturated to a limited value. This limitation can dramatically change the system dynamics, for example, forcing a chaotic system to oscillation quenching. This is also important for various natural and man-made systems, ranging from climate, lasers, chemistry, and engineering systems. Moreover, we find that the amplitude constraint induced OD is not exclusive in coupled chaotic systems, such as the coupled Lorenz oscillators with two different coupling manners as reported in the paper; it also appears in coupled periodic systems such as the Landau-Stuart oscillators.

In the paper, the odd function property of the nonlinear function is required for the theoretic analysis. It is unclear whether this limitation can be removed. In addition, the problem whether the amplitude constraint effect is helpful to revive oscillations [44] is interesting and needs further research.

ACKNOWLEDGMENTS

W.L. was supported by the National Natural Science Foundation of China (NSFC) (Grants No. 11262006 and No. 11405075), the postdoctor project of China (Grant No. 2014M552122), the project of high school of Jiangxi province (Grant No. KJLD14047), and the training plan of young scientists of Jiangxi province. Zhan was supported by the NSFC under Grant No. 11475253.

[1] Y. Kuramoto, *Chemical Oscillations, Waves, and Turbulence* (Springer, Berlin, 1984).
[2] M. Lakshmanan and D. V. Senthilkumar, *Dynamics of Nonlinear Time-Delay Systems* (Springer, Berlin, 2010).
[3] S. Boccaletti, J. Kurths, G. Osipov, D. L. Valladares, and C. Zhou, Phys. Rep. **366**, 1 (2002).
[4] L. M. Pecora and T. L. Carroll, Phys. Rev. Lett. **64**, 821 (1990).
[5] M. G. Rosenblum, A. S. Pikovsky, and J. Kurths, Phys. Rev. Lett. **76**, 1804 (1996).
[6] W. Liu, J. Xiao, X. Qian, and J. Yang, Phys. Rev. E **73**, 057203 (2006).
[7] G. Saxena, A. Prasad, and R. Ramaswamy, Phys. Rep. **521**, 205 (2012).
[8] A. Koseska, E. Volkov, and J. Kurths, Phys. Rep. **531**, 173 (2013)
[9] A. Koseska, E. Volkov, and J. Kurths, Phys. Rev. Lett. **111**, 024103 (2013).
[10] G. Song, N. V. Buck, and B. N. Agrawal, Journal of Guidance, Control, and Dynamics **22**, 433 (1999).
[11] E. Ullner, A. Zaikin, E. I. Volkov, and J. Garcia-Ojalvo, Phys. Rev. Lett. **99**, 148103 (2007).
[12] A. Koseska, E. Volkov, and J. Kurths, Europhys. Lett. **85**, 28002 (2009).
[13] M. Y. Kim, R. Roy, J. L. Aron, T. W. Carr, and I. B. Schwartz, Phys. Rev. Lett. **94**, 088101 (2005).
[14] A. Prasad, Y. C. Lai, A. Gavrielides, and V. Kovanis, Phys. Lett. A **318**, 71 (2003).
[15] I. Grosu, E. Padmanaban, P. K. Roy, and S. K. Dana, Phys. Rev. Lett. **100**, 234102 (2008).
[16] Y. Zhai, I. Z. Kiss, and J. L. Hudson, Phys. Rev. E **69**, 026208 (2004).
[17] A. Koseska, E. Ullner, E. Volkov, J. Kurths, and J. García Ojalvo, J. Theor. Biol. **263**, 189 (2010).
[18] N. Suzuki, C. Furusawa, and K. Kaneko, PLoS ONE **6**, e27232 (2011).
[19] C. R. Hens, O. I. Olusola, P. Pal, and S. K. Dana, Phys. Rev. E **88**, 034902 (2013).
[20] W. Liu, E. Volkov, J. Xiao, W. Zou, M. Zhan, and J. Yang, Chaos **22**, 033144 (2012).
[21] G. B. Ermentrout, Phys. D (Amsterdam, Neth.) **41**, 219 (1990).
[22] W. Liu, J. Xiao, L. Li, Y. Wu, and M. Lu, Nonlinear Dynamics **69**, 1041 (2012).
[23] J. Yang, Phys. Rev. E **76**, 016204 (2007).
[24] Z. Hou and H. Xin, Phys. Rev. E **68**, 055103 (2003).
[25] W. Liu, X. Wang, S. Guan, and C. H. Lai, New J. Phys. **11**, 093016 (2009).
[26] H. Bi, X. Hu, X. Zhang, Y. Zou, Z. Liu, and S. Guan, Europhys. Lett. **108**, 50003 (2014).
[27] R. E. Mirollo and S. H. Strogatz, J. Stat. Phys. **60**, 245 (1990).
[28] H. Ma, W. Liu, Y. Wu, M. Zhan, and J. Xiao, Commun. Nonlinear Sci. Numer. Simul. **19**, 2874 (2014).
[29] Y. Wu, W. Liu, J. Xiao, W. Zou, and J. Kurths, Phys. Rev. E **85**, 056211 (2012).
[30] R. Karnatak, R. Ramaswamy, and A. Prasad, Phys. Rev. E **76**, 035201(R) (2007).
[31] Y. Zhu, X. Qian, and J. Yang, Europhys. Lett. **82**, 40001 (2008).
[32] K. Konishi, Phys. Rev. E **68**, 067202 (2003).
[33] D. V. Ramana Redy, A. Sen, and G. L. Johnston, Phys. Rev. Lett. **80**, 5109 (1998).
[34] F. M. Atay, Phys. Rev. Lett. **91**, 094101 (2003).
[35] W. Zou, D. V. Senthilkumar, A. Koseska, and J. Kurths, Phys. Rev. E **88**, 050901(R) (2013).
[36] S. H. Strogatz, Nature (London) **394**, 316 (1998).
[37] M. G. Crosby, US Patent No. 2276565, 1942.
[38] A. Takada and W. Imajuku, Electron. Lett. **32**, 677 (1996).
[39] J. Gao and J. Peng, Chin. Phys. Lett. **24**, 1614 (2007).
[40] X. Zhang and K. Shen, Phys. Rev. E **63**, 046212 (2001).
[41] G. Hu, J. Yang, and W. Liu, Phys. Rev. E **58**, 4440 (1998).
[42] J. Menck, J. Heitzig, N. Marwan, and J. Kurths, Nat. Phys. **9**, 89 (2013)
[43] E. Sanchez and M. A. Matias, Phys. Rev. E **57**, 6184 (1998).
[44] W. Zou, D. V. Senthilkumar, M. Zhan, and J. Kurths, Phys. Rev. Lett. **111**, 014101 (2013).